npj | clean water

www.nature.com/npjcleanwater

ARTICLE OPEN

Check for updates

Succession of bacterial biofilm communities following removal of chloramine from a full-scale drinking water distribution system

Tage Rosenqvist[1,2], Mikael Danielsson[1,2,3], Caroline Schleich[4], Jon Ahlinder[5], Björn Brindefalk[5], Kristjan Pullerits[1,2], Ingrid Dacklin[5], Emelie N. Salomonsson[5], David Sundell[5], Mats Forsman[5], Alexander Keucken[4], Peter Rådström[1] and Catherine J. Paul[1,6]✉

Monochloramine is used to regulate microbial regrowth in drinking water distribution systems (DWDS) but produces carcinogenic disinfection byproducts and constitutes a source of energy for nitrifying bacteria. This study followed biofilm-dispersed microbial communities of a full-scale DWDS distributing ultrafiltered water over three years, before and after removal of monochloramine. Communities were described using flow cytometry and amplicon sequencing, including full-length 16S rRNA gene sequencing. Removal of monochloramine increased total cell counts by up to 440%. Increased abundance of heterotrophic bacteria was followed by emergence of the predatory bacteria *Bdellovibrio*, and a community potentially metabolizing small organic compounds replaced the nitrifying core community. No increased abundance of *Mycobacterium* or *Legionella* was observed. Co-occurrence analysis identified a network of *Nitrosomonas*, *Nitrospira*, *Sphingomonas* and *Hyphomicrobium*, suggesting that monochloramine supported this biofilm community. While some species expanded into the changed niche, no immediate biological risk to consumers was indicated within the DWDS.

npj Clean Water (2023)6:41 ; https://doi.org/10.1038/s41545-023-00253-x

INTRODUCTION

One strategy to limit bacterial regrowth in drinking water distribution systems (DWDS) is the application of a secondary disinfectant. The disinfectant generally used has been chlorine, due to its efficiency in reducing concentrations of heterotrophs[1], which are considered indicators of microbial drinking water quality[2]. Demands for higher chemical stability have led to replacement of free chlorine with monochloramine (MCA), which can inhibit growth in more remote areas of the DWDS[3] and generates fewer regulated disinfection byproducts[4]. However, the chemical stability of MCA is negatively affected by reactions with biomass as well as cometabolization of MCA with ammonium by nitrifying microorganisms[5–7]. Nitrification is an undesirable phenomenon in DWDS, as it can lead to potentially hazardous concentrations of nitrite and nitrate. Due to these factors as well as concerns regarding the formation of carcinogenic disinfection byproducts[8], several European drinking water producers have chosen to forgo secondary disinfection entirely[9].

Biological nitrification is typically driven by ammonia oxidizing bacteria (AOB) and nitrite oxidizing bacteria (NOB). AOB convert ammonia to nitrite, while NOB convert nitrite to nitrate. The energy provided is then used to fix inorganic carbon. In chloraminated DWDS, AOB generally belong to genera *Nitrosomonas* and *Nitrosospira*, while NOB belong to genus *Nitrospira*[10]. Some *Nitrospira* can also convert ammonia directly to nitrate (comammox)[11]. Nitrifying bacteria co-exist with heterotrophic bacteria, which benefit from the carbon produced by nitrifiers[12] while the nitrifiers benefit from the production of biofilm and consumption of inhibitory metabolites by heterotrophs[13].

Over 98% of the biomass in DWDS is thought to be present within biofilm attached to the pipe walls rather than the bulk water[14]. Studying this fraction within full-scale DWDS is challenging as it requires the excavation of pipes. In addition, analysis of the dispersal of microorganisms from the biofilm into the bulk water is masked in most DWDS by the presence of taxa originating from the source water and processes within the drinking water treatment plant (DWTP)[15,16]. Recently, introduction of a coagulation-ultrafiltration hybrid step in a full-scale Swedish DWTP resulted in the complete removal of bacterial cells from the DWDS to reveal bacteria entering the chloraminated water from biofilm, as well as those in surface and deep biofilm from excavated pipes. The dominant genera in the core pipe biofilm community were identified as *Nitrosomonas*, *Nitrospira*, *Sphingomonas* and *Hyphomicrobium*[17]. Similar communities have been observed in other chloraminated systems, although not specifically localized to biofilm[18,19].

The diverse nature of DWDS microbial communities as well as technical limitations can lead to a focus[20–22] on the most abundant and prevalent taxa. While a small number of abundant taxa may explain major trends in a dataset[23], this approach omits rare microorganisms. Members of the rare biosphere, defined as those which are in low abundance or abundant under specific circumstances, have been shown to play significant roles in many microbial communities, functioning as keystone organisms and microbial seed banks[24]. When operational parameters were changed to promote nitrification in a simulated chloraminated DWDS, conditionally rare taxa became abundant, and subsequently returned to their rare status, as the system was restored[25]. That specific changes in drinking water production and

[1]Division of Applied Microbiology, Department of Chemistry, Lund University, P.O. Box 124, SE-221 00 Lund, Sweden. [2]Sweden Water Research AB, Ideon Science Park, Scheelevägen 15, SE-223 70 Lund, Sweden. [3]Norrvatten, Vattenverksvägen 20, SE-175 47 Järfälla, Sweden. [4]Vatten & Miljö i Väst AB, SE-311 22 Falkenberg, Sweden. [5]FOI, Swedish Defense Research Agency, Cementvägen 20, SE-906 21 Umeå, Sweden. [6]Water Resources Engineering, Department of Building and Environmental Technology, Lund University, SE-221 00 Lund, Sweden. ✉email: catherine.paul@tvrl.lth.se

distribution could result in recruitment of taxa from the rare biosphere and have serious implications for human health if conditions were such that a sudden emergence of pathogenic taxa sequestered in biofilm occured[26].

This study examined the response of bacterial communities dispersed from biofilm in a full-scale DWDS to the removal of chloramination from the treatment process. As the water is ultrafiltered prior to distribution, no cells in this DWDS can originate from the source water or treatment process. Previous studies have shown that the bulk water communities mirror those in the biofilm of this system[17], and thus all cells present in the drinking water originate from biofilm communities[27]. The biofilm communities of this DWDS are though to play a significant role in nitrification and chloramine decay[17], and it was not known how these communities would respond as chloramination ended, and whether there would be changes that could relate to microbial health risk. Changes in community dynamics immediately following the end of chloramination, and for 2 years after, were investigated to assess short- and long-term community shifts due to changing environmental conditions.

RESULTS AND DISCUSSION

Upstream disinfection determines response of DWDS biofilm

Total cell counts (TCC) and intact cell counts (ICC) were available from the 2 years prior (2018, 2019) and 2 years following (2020, 2021) the end of chloramination. Data was selected from six sampling points to represent a gradient of disinfectant concentrations in the DWDS (Fig. 1a) in order to quantify the growth limiting effects of MCA, however, flow cytometry (FCM) data was not available for Distribution Point South 1 (DPS1), which was sampled for DNA sequencing sampling.

Comparison of TCC after the end of chloramination, in 2020 and 2021, to a baseline model generated using data from 2018 to 2019 revealed increased cell counts at all points (Fig. 1b). Chow tests identified highly statistically significant structural breaks induced by the change in chloramination for all points ($F = 21.7–213$, $p < 0.01$), except for DPS3, where the break was not significant ($F = 3.00$, $p = 0.0354$). The highest TCC increase compared to the baseline was at DPS2, with an increase of 38600 ± 2060 cells/ml. This was significantly higher than that for any other sampling point ($W = 1437$ to 1960, Holm- adjusted $p < 0.01$, pairwise Wilcoxon rank-sum test). Downstream from DPS2, the TCC at DPS3 increased by 7860 ± 4070 cells/ml, a significantly smaller increase than the other DWDS points ($W = 50–335$, Holm-adjusted $p < 0.01$, pairwise Wilcoxon rank-sum test). The TCC increases at DPE, DPN and DPW were between 16,600 and 17,700 cells/ml and were not significantly different from each other ($W = 697–830$, Holm-adjusted $p > 0.8$, pairwise Wilcoxon rank-sum test). At the WTP, TCC increased by 1820 ± 170 cells/ml, a significantly smaller increase than at all other points except DPS3 ($W = 0–147$, Holm-adjusted $p < 0.01$, pairwise Wilcoxon rank-sum test). Expressed as relative increases in TCC following removal of chloramine, the largest relative increase occurred at DPW (+440%), followed by WTP (+438%), DPN (+252%), DPS2 (+196%), DPE (+33.7%) and DPS3 (+6.92%). ICC showed the same pattern (Supplementary Fig. 1), likely due to the high degree of correlation between the measurements (Pearson correlation coefficient of 0.991 ± 0.00162, $p < 0.05$). Linear regression of ICC as a function of TCC provided a good fit ($R^2 = 0.982$), with a slope of 0.678 ± 0.00764 and a non-significant intercept of 459 ± 46200 ($p > 0.05$). This suggests that on average 67.8% of the observed cells were intact.

The growth suppressing activity of MCA on DWDS biofilm is dose dependent[28,29], however previous studies have mainly studied disinfection gradients across a DWDS. The current study allowed examination of the rebound of growth following removal at individual locations and while the largest relative TCC increases occurred where the MCA concentrations were previously the highest (WTP, DPW), the largest absolute TCC increase observed after the end of chloramination was downstream of the location with high relative increases, at DPS2. That the absolute TCC increase was highest downstream, and not at the points with previously high MCA concentrations, can be explained by the combined effects of accumulation of cells from continual contact with biofilm, and increased growth permitted both from biofilm and the cells release from the biofilm into the water after the end of chloramination. MCA continuously decays through biological and chemical mechanisms, so concentrations were highest at points with low residence times and consequently, the sections of upstream biofilm where growth was suppressed were smaller at WTP and DPW than those further out into the DWDS, such as DPS2. That DPS3 experienced a smaller increase in TCC than DPS2 can be explained also by distance, with longitudinal dispersion diluting the increase of cells due to removal of chloramine. Understanding the relationship of TCC to hydraulic characteristics in the DWDS would be useful to predict the response in DWDS where MCA would be removed, to ensure accurate interpretations of changes, or lack of changes, in cell counts during transition to a disinfectant-free DWDS.

Despite increased cell counts at all points, it was noted that the concentration of organic matter (measured as chemical oxygen demand) was relatively constant over the course of the study (Supplementary Table 5), attesting to the difficulty of observing these changes through monitoring of conventional water quality parameters.

The impact of ending chloramination on the composition of the microbial community in the water was investigated by sequencing the V3-V4 region of the 16S rRNA gene using Illumina MiSeq. While no sequences were obtained for WTP, DPS3 and DPW due to technical issues and budget constraints (see Methods), the sequenced sampling locations still represented a gradient of chloramination for investigation. Historical MCA concentrations influenced the degree to which the bacterial community composition changed in response to the end of chloramination (Fig. 2). Beta-dispersion of the communities at each sampling point indicated significantly lower dispersion in DPE than at other points ($t = -12.7$ to -4.68, $p < 0.01$, pairwise permutation-based test), while the dispersion at DPN was significantly higher ($t = 5.75–12.7$, $p < 0.01$, pairwise permutation-based test), showing that the community at DPN underwent especially significant phylogenetic shift following the end of chloramination, while DPE was least affected. It was necessary to rule out seasonal fluctuations[30,31] as an explanation for the differences in communities, and as the communities on the first two sampling occasions were subjected to MCA, but experienced different temperatures (10.6 ± 1.68 °C in October 2019 vs 8.15 ± 0.806 °C in December 2019) were not significantly different ($F = 1.32$, $p = 0.282$, PERMANOVA), this supported that the observed changes were due to the presence or absence of MCA.

The biofilm community shifts from autotrophy to heterotrophy

Core communities are defined as taxa present at many or all points sampled in a specific environment, and the microorganisms in the core are likely to be fundamental in ensuring the survival of the larger community[32]. In this study, the initial core community of the DWDS, defined as taxa detected at all sampling locations before the end of chloramination, was primarily composed of genera *Nitrosomonas*, *Nitrospira*, *Sphingomonas* and *Hyphomicrobium*, constituting 25–80% of the total bacterial community at the various sampling locations (Fig. 3a). The relative abundance of the core community was highest at DPN (81.9–87.9%) and lowest at DPE (26.4–32.7%), with intermediate relative abundance at DPS1 (40.7–49.1%) and DPS2 (45.3–50.9%). Co-occurrence analysis

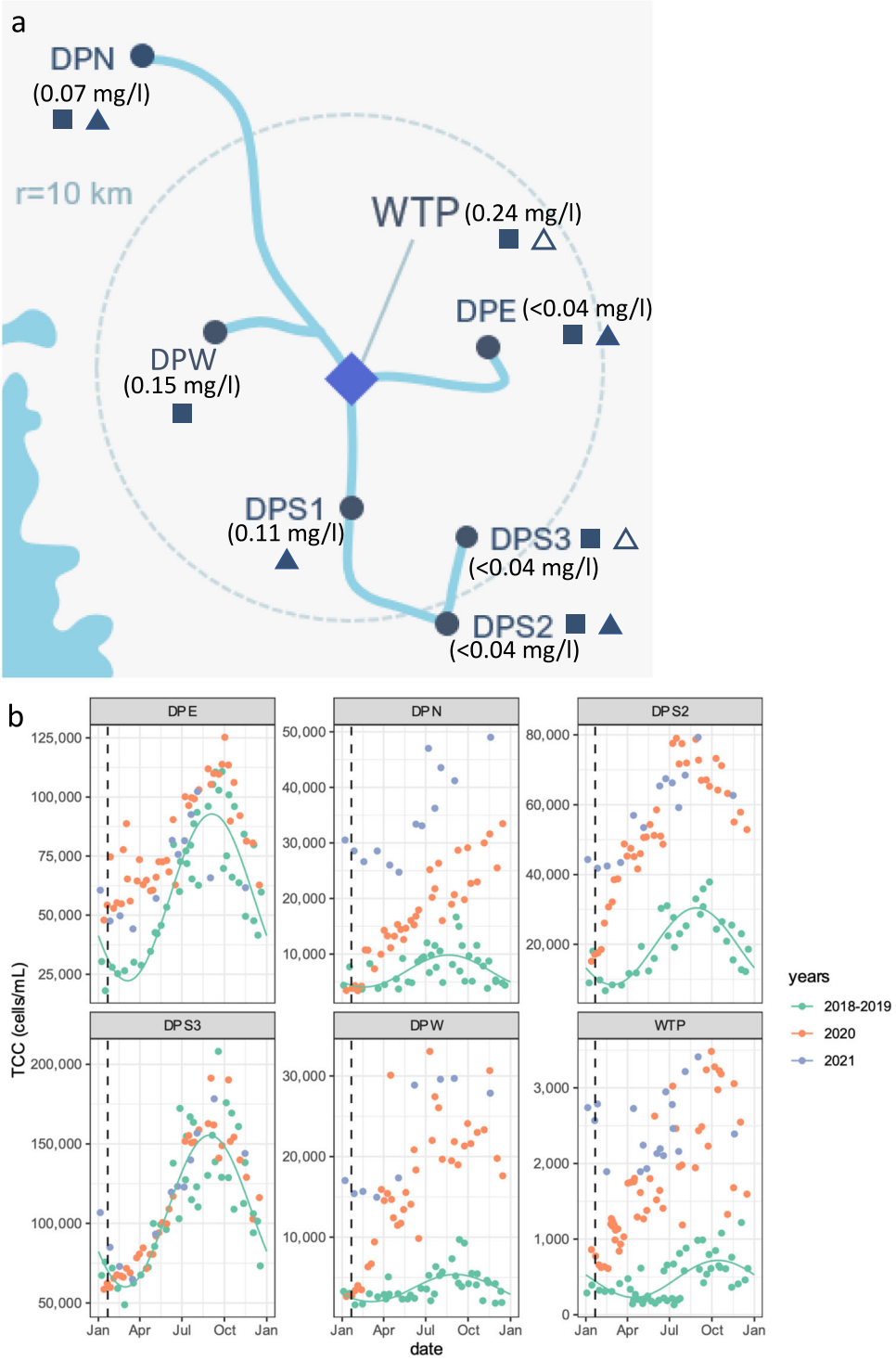

Fig. 1 DWDS sampling points and total cell counts before and after removal of MCA. a Map of the DWDS showing sampling points and chlorine concentrations prior to end of chloramination. Distribution points (DP) were named with a suffix to indicate their cardinal direction in relation to the DWTP. The southern distribution points (DPS1-3) are downstream of each other, and numbered with respect to their distance from the DWTP (1 is closest). ■ = FCM data available, ▲ = samples taken for sequencing, △ = samples taken for sequencing but not included in bioinformatics analysis (see Methods). **b** Total cell concentrations measured before and after the end of chloramination. Points represent measured TCC values. The solid line shows the modeled variation due to seasonal effects prior to the end of chloramination. The dashed, vertical line indicates when chloramination ended (January 20th, 2020).

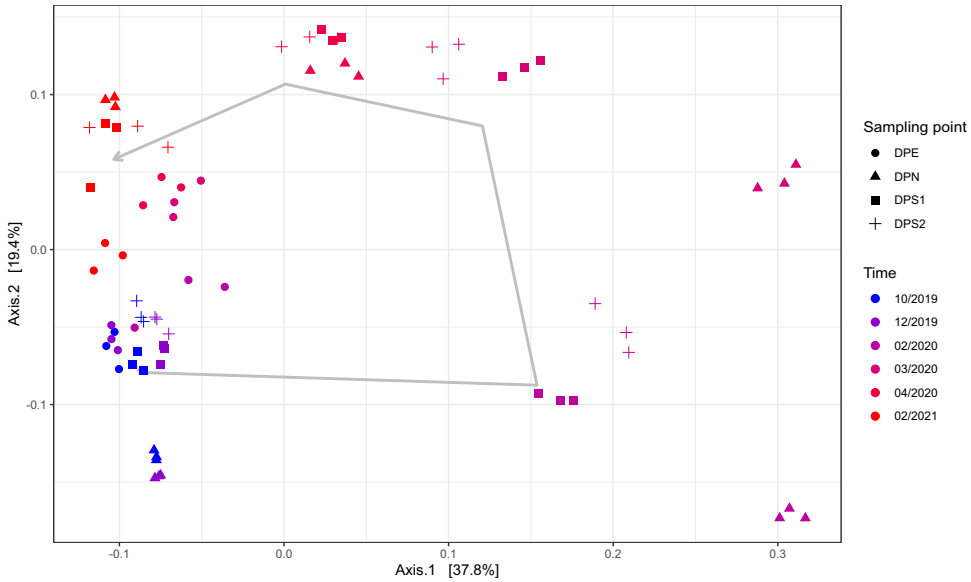

Fig. 2 Principal coordinates analysis (PCoA) of DWDS samples with weighted unifrac distances. The arrow marks the mean coordinates of all sampling points at each timepoint to highlight the transition of the bacterial communities over time.

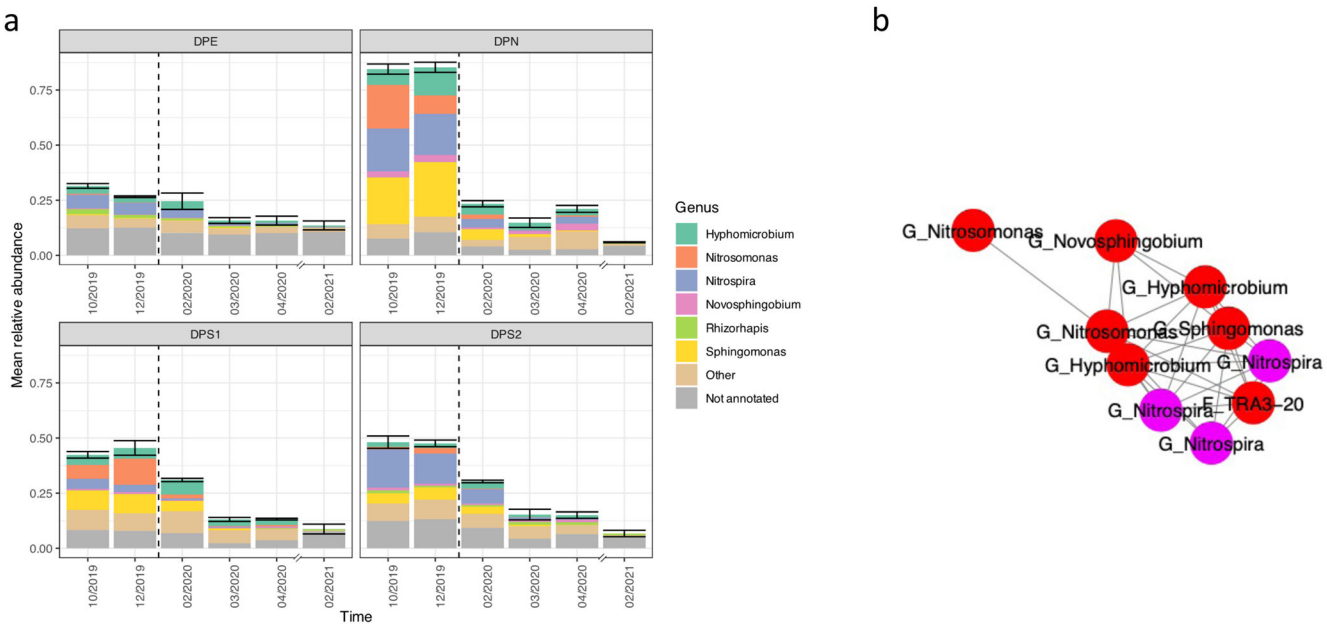

Fig. 3 Identity and relationships in the biofilm community before MCA removal. a Relative abundance of the initial core community. Each bar represents the average of three biological replicates. Error bars represent standard deviations for the total relative abundance of this core community ($n = 3$ at each sampling location and time). The dashed, vertical line represents the end of chloramination. Note that the x-axis is not to scale: the final samples were taken 10 months after the penultimate samples. **b** Co-occurrence network showing nodes representing ASVs potentially involved in MCA metabolism. Shown is a component which included ASVs identified as core taxa, selected visually from the full co-occurrence network (Supplementary Fig. 3). Edges represent strong (Spearman's rho > 0.75) and significant (Holm-adjusted $p < 0.01$) correlations in TCC scaled abundance. The nodes represent ASVs and are colored by class (red = Alphaproteobacteria, purple = Nitrospiria).

showed that the abundances of some amplicon sequence variants (ASVs) within *Nitrosomonas*, *Nitrospira*, *Sphingomonas* and *Hyphomicrobium* had strong (Spearman's $|\rho| > 0.75$) and significant ($t > 9.52$, Holm-adjusted $p < 0.01$) correlations with each other (Fig. 3b).

The high relative abundance of core community taxa in DPN explains the low diversity observed at this sampling point before chloramination was ended (Supplementary Fig. 2). The section of pipe leading to DPN has a high flow rate and MCA concentration, which have previously been associated with low diversity[33,34] due to selection for adhesive and MCA-resistant organisms. *Nitrosomonas*, *Nitrospira*, *Sphingomonas* and *Hyphomicrobium* have previously been reported in several chloraminated systems[17–19], although definite metabolic interactions between their members have not been observed. However, as the relative abundances of these core community members decreased after the end of chloramination, and the co-occurrence analysis identified strong and significant correlations among some ASVs of the core community, this suggested that these genera could from a cooperative consortium involved in the metabolization of MCA.

Identification at species-level with full-length 16S rRNA sequences from DPS1 provided a link between taxa with known roles in nitrification and the hypothesis that the core community present before the end of chloramination was supported by the presence of MCA. *Nitrosomonas sp*. Is79 was the most abundant identified member of the genus *Nitrosomonas* (Supplementary Table 1), representing over 95% of the relative abundance of the genus *Nitrosomonas Sp*. Is79 thrives at low concentrations of ammonium and has been isolated from freshwater[35] and a member of genus *Nitrosomonas*, *N. europaea*, can cometabolize MCA at drinking water concentrations[6]. This suggests that *N. sp* Is79 could decay MCA to nitrite in this DWDS and serve as a primary producer of organic carbon by CO_2 fixation. The possible competitive advantage afforded by MCA cometabolism might explain the higher relative abundance of *Nitrosomonas* observed at the sampling points in this study with the highest concentrations of MCA (DPS1, DPN).

The predominant *Nitrospira* species identified were *N. lenta*, *N. japonica* and *N. moscoviensis* (Supplementary Table 1) comprising over 85% of this genus at DPS1, with the exception of *N. defluvii*, a member of sublineage I, which increased up to a relative abundance of 28.9% of the total *Nitrospira* immediately after the end of chloramination (02/2020). The presence of *N. inopinata*, notable for its ability to perform comammox[11], was detected as a minor component (4.47–7.77%) in all samples. *N. lenta*, *N. japonica* and *N. moscoviensis* are all part of *Nitrospira* sublineage II, associated with low nitrate and high oxygen concentrations[36,37]. The growth of the more oxygen-sensitive *N. defluvii*[38,39] over sublineage II *Nitrospira* following the end of chloramination may have been favored if lower oxygen concentrations in the pipe biofilm were a result of heightened activity of aerobic heterotrophs such as *Bacteroides* (see below). Comammox bacteria have previously been shown to be present alongside canonical ammonium oxidizers in DWDS[40,41]. While cometabolism of MCA by comammox bacteria has not yet been demonstrated, the increased resolution provided by the full-length 16S sequences suggests specific members of the genus *Nitrospira* are participating in MCA metabolism via nitrite oxidation, and possibly ammonium oxidation via commamox. They may also provide organic carbon by CO_2 fixation, and their potential role in cometabolism of MCA cannot be excluded. In a previous study of this DWDS, *Nitrosomonas* dominated pipe biofilm communities upstream from biofilm that was highly abundant in *Nitrospira*, which would be consistent with a conversion of ammonia to nitrite as water flowed through the pipe[17].

A diverse community of *Sphingomonas* species was observed at DPS1, with abundant species including *S. alpina*, *S. desiccabilis* and *S. zeicaulis* (Supplementary Table 1). With diverse metabolic capabilities, it is difficult to identify the specific roles of this genus to MCA metabolism in this system, as few studies exist of specific nonpathogenic strains in a drinking water context. In general, genus *Sphingomonas* is composed of aerobic chemoheterotrophs, with two species also capable of photoorganotrophy[42]. They are proficient at metabolizing complex and recalcitrant organic compounds[43], in particular chlorinated organic molecules[44], and they could thus metabolize high molecular weight compounds produced by autotrophs oxidizing MCA, and present in the bulk water. The capability of *Sphingomonas* to degrade chlorinated organic compounds may be related to the resistance of some strains to free chlorine[45]. This genus has been implicated in initiation and maturation of biofilms on reverse osmosis membranes for drinking water production[46], owing to their significant production of exopolysaccharides (EPS)[47].

Heterotrophic EPS has proven to be important in the formation of nitrifying biofilms[48]. In addition, by producing CO_2 as the product of respiration it can potentially promote the growth of carbon-fixing autotrophs in the biofilm. Lastly, the production of EPS can serve to establish and maintain the biofilm.

The dominant species of *Hyphomicrobium* in this DWDS were *H. nitrativorans* and *H. sp. MC1* (Supplementary Table 1), which together represented over 70% of the abundance of the genus in DPS1. Genus *Hyphomicrobium* contains members capable of living in anaerobic drinking water biofilms using of nitrate and nitrite as electron acceptors[49] and aerobic metabolisms in drinking water biofilms can generate these environments[50]. Aside from their capabilities of denitrification, *Hyphomicrobium* lack pyruvate carboxylase, restricting their metabolism to organic molecules with two carbon atoms or less[51]. *H. nitrativorans* has been shown to be capable of complete denitrification[49], while *H. sp. MC1* is can degrade chloromethane[52]. This indicates that the *Hyphomicrobium* species present in the DWDS biofilm could grow aerobically as well as anaerobically by metabolizing low molecular weight organic compounds present in the bulk water, using nitrate produced by the autotrophs as an electron acceptor and potentially produce high molecular weight compounds for use by *Sphingomonas* species.

A model for MCA metabolism in drinking water biofilms

Combining species level information from full-length 16S rRNA gene sequencing with the interactions suggested by co-occurrence network analysis, a microbial food web for the metabolization of MCA can be proposed (Fig. 4). Similar tightly interlinked autotroph-heterotroph microbial communities can be observed within nitrifying granules for wastewater treatment[53], albeit with taxa adapted to higher ammonium concentrations. This could be useful for simulating nitrification processes in DWDS, if coupled with a physico-chemical model taking into account chemical reactions, diffusion processes and mobilization phenomena, such as what has recently been suggested for carbon cycling[54]. Metagenomic sequencing, targeted qPCR assays to specific genes and/or constructing synthetic DWDS biofilm communities containing these taxa can further enhance our understanding of the dynamics of biological MCA decay. This approach has been applied to analyze plant[55] and gut[56] microbiomes but not yet in drinking water contexts. Although the flow cytometry data indicated that most cells (67.8%) observed in the system were intact and thus likely metabolically active, it is in theory possible that the observed taxa are in the membrane-permeated minority. As such, RNA sequencing could be applied to conclusively identify the active members of the DWDS microbial community, and to confirm or revise the model.

MCA removal reveals predator-prey relationships within DWDS

With metabolism of the initial core community linked to MCA, it was anticipated that following the end of chloramination, a new bacterial community would emerge that would use alternative food webs to benefit from the disinfectant-free environment.

To examine the community transition, taxa identified by the V3-V4 16S rRNA gene sequencing were compared over time and at individual sampling points. Since clear variations in microbial load were present (Fig. 1b), normalization was applied to the compositional sequencing data by scaling the relative abundances of each with the TCC measured at the same sampling point and time (Fig. 5).

The abundance of class *Bacteroidia* increased at all sampling locations in the DWDS following the end of chloramination. *Bacteroidia* became over 2000 times more abundant at DPN and immediately following the end of chloramination, *Bacteroidia* was the dominant class at DPN, DPS1 and DPS2. This class was primarily represented by the genus *Flavobacterium* and two largely uncultured families within the order *Sphingobacteriales*: *env.OPS 17*, and *KD3−93* (Supplementary file 1). Full-length 16S gene amplicons sequenced from DPS1 provided species level classifications and resolved *Flavobacterium terrigena* as the most

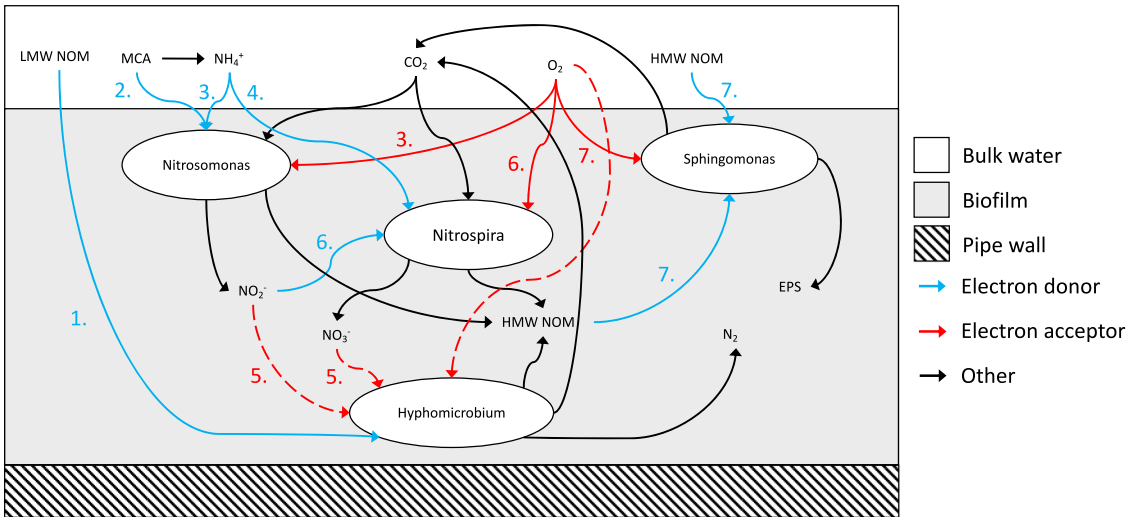

Fig. 4 Conceptual model of an MCA-metabolizing food web. Dashed lines represent the potential possibility for *Hyphomicrobium* to utilize several different electron acceptors. Numbers in the figure refer to studies wherein the capability to use given electron donor/acceptor has been shown experimentally for the indicated genus: 1. [105], 2. [6], 3. [106], 4. [11], 5. [49], 6. [107], 7. [108].

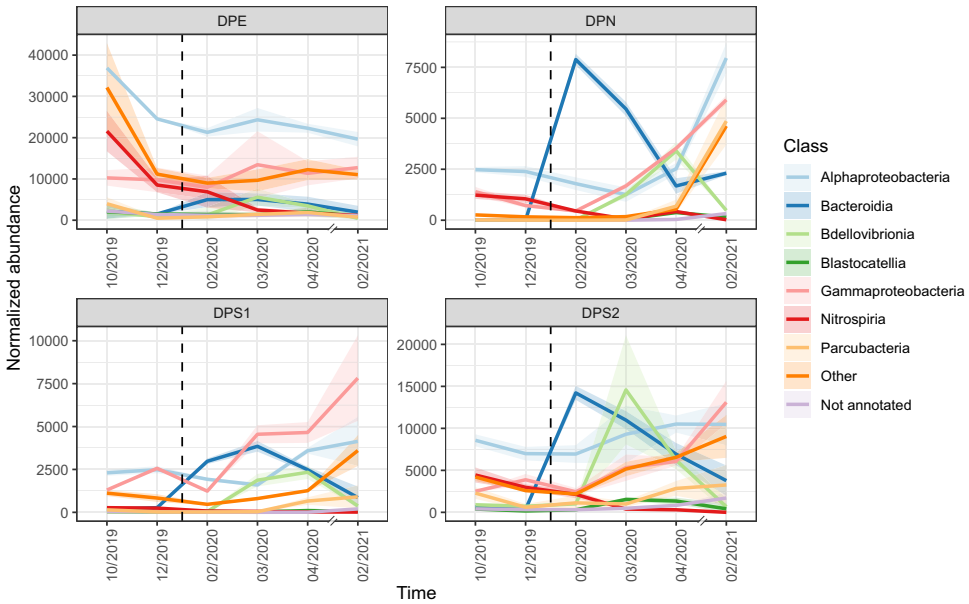

Fig. 5 Normalized abundance of the most abundant classes within the DWDS. The dashed, vertical line represents the end of chloramination. Shaded areas represent 90% confidence intervals, assuming a normal distribution of replicate values at each time point ($n = 3$ at each sampling location and time). Note that the x-axis is not to scale: the final samples were taken 10 months after the penultimate samples.

abundant member of genus *Flavobacterium* at this location (Supplementary Table 2).

Class *Bacteroidia* is part of the phylum *Bacteroidota*, which is associated with degradation of complex biopolymers and periods of intense heterotrophic activity in the time after cyanobacterial blooms in freshwater[57]. In this DWDS, routine monitoring by the utility indicated high heterotrophic activity in the form of a temporary increase in heterotrophic plate counts following the end of chloramination, where threshold values of 100 colony forming units/ml were briefly exceeded in DPW[58]. Two representatives of the family *env.OPS17*, identified in this study by full length sequencing, were recently cultured and determined to exclusively prefer complex carbon sources[59], and *Flavobacterium* species have been shown to utilize a variety of polysaccharides even at very low concentrations[60,61]. The common preference for high molecular weight organic matter, and association with intense heterotrophic growth, could explain the increase of *Bacteriodia* observed here. These bacteria would have been no longer suppressed by disinfection, allowing them to flourish using the organic matter present within the DWDS biofilm. While this DWDS is fed with drinking water that has been subjected to a combined coagulation/ultrafiltration to remove cells and organic matter, *Bacteroidia* from drinking water have been shown to proliferate when provided with dead bacterial cells as nutrition[21]. As *Nitrospira* and other bacteria linked to metabolism of MCA would be dying off, this biomass (necromass) would have been available in this system, allowing growth of these *Bacteroidia* species to exceed those of more oligotrophic heterotrophs, and become the dominant heterotrophs for some time.

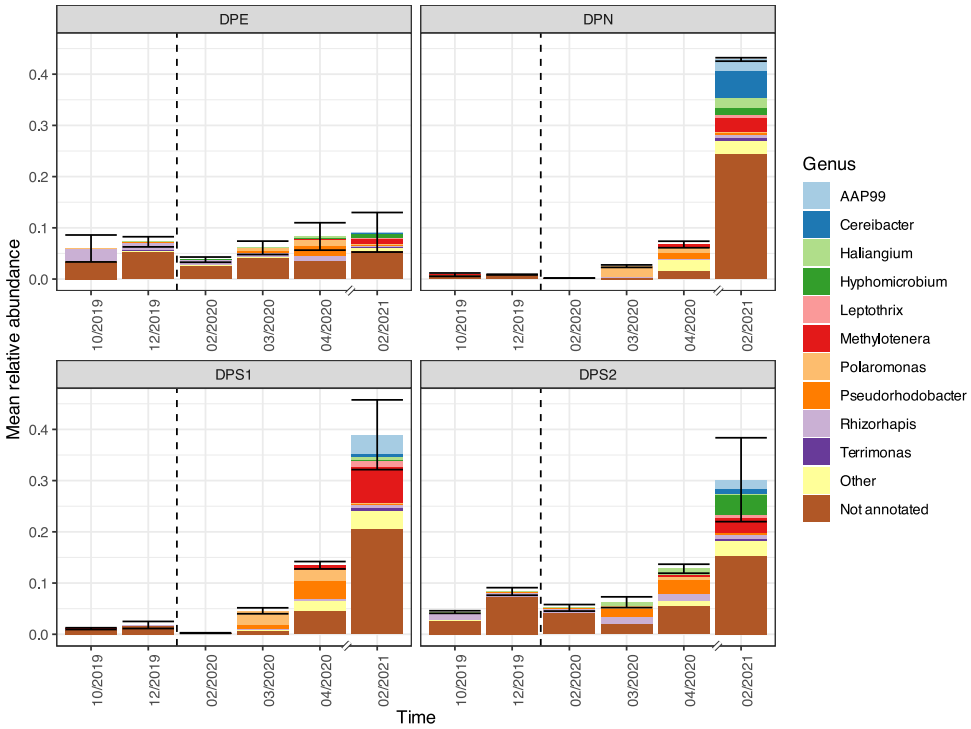

Fig. 6 Relative abundance of the post-MCA core community. The dashed, vertical line represents the end of chloramination. Error bars represent standard deviations for the total relative abundance of the MCA-adapted core community ($n = 3$ at each sampling location and time). Note that the x-axis is not to scale: the final samples were taken 10 months after the penultimate samples.

An increase in class *Bdellovibrionia* was observed following the increased abundance of *Bacteroidia* at all DWDS points and was dominated by members of the type genus *Bdellovibrio* (Supplementary file 1). Full-length 16S sequencing from DPS1 identified the type species *B. bacteriovorus* as the most abundant member of the genus before the end of chloramination, while later time points (03/2020 and 04/2020) were dominated by *B. exovorus* (Supplementary Table 2). *Bdellovibrionia* is composed of predatory bacteria with various host specificities[62]. The life cycle of *B. bacteriovorus* is complex, consisting of a free-living attack phase, in which Gram-negative prey is located, followed by a period of replication within the periplasm and the eventual lysis of the prey cell[63]. In contrast, *B. exovorus* does not enter the periplasm but instead attaches to the outside of the prey cell[64]. While little is known about the role of *Bdellovibrio* in drinking water, successful use of *B. bacteriovorus* as a biological control agent against biofilm has been demonstrated[65], suggesting it could have a similar role in control of growth in DWDS biofilms. Co-culture experiments have shown that the predator-prey relationship of *Bdellovibrio* and their prey closely follow the Lotka-Volterra model of interactions[66] and as this is similar to what was observed here, with *Bdellovibrio* emerging as class *Bacteroidia* become less abundant, this suggests that there is a predator-prey relationship between these two taxa in drinking water. Classes *Bacteroidia* and *Bdellovibrionia* have not been detected in previous studies of this DWDS, where biofilm communities sampled by swabs and scrapes of pipe surfaces, and water communities, were described[17]. This indicates that these are conditionally rare taxa which became abundant when environmental conditions, in this case the removal of chloramine, were permissive. Growth of *Bacteroidia* can be explained by both the lack of growth suppression and the abundance of dead nitrifier bacteria, while *Bdellovibrionia* could benefit from this increased prey density. A relationship between prevalence of *Bdellovibrio* and lack of secondary disinfection has also been observed in other DWDS, as a global meta-analysis showed higher abundance and prevalence of *Bdellovibrio* in DWDS without secondary disinfectant[67].

Examining changes in abundance of pathogens

That specific taxa originating from biofilm can rapidly increase in numbers when environmental changes occur is of special concern given that biofilm has been proposed as a reservoir for pathogenic bacteria[26]. Coupled with the removal of secondary disinfection, and increases in TCC (Fig. 1b) it was important to examine if there were any indications of increased abundance of known water-borne pathogens in this DWDS following removal of MCA, as abnormal changes in cell concentrations are considered indicators of potential risk in the EU directive on the quality of water intended for human consumption[68]. While many opportunistic pathogens have been described for drinking water[26], sequences identified as genera *Mycobacterium* or *Legionella* had been previously detected in this DWDS[17]. Normalized abundances of these genera, however, did not increase in the long or short term, and these taxa were present at very low levels throughout the study (Supplementary Fig. 4). The TCC-normalized abundance of *Mycobacterium* was significantly higher in the samples taken before chloramination was ended at all DWDS points (Wilcoxon rank-sum test, Holm-adjusted $p < 0.01$) (Supplementary Table 3), mirroring observations of increased *Mycobacterium* abundance when MCA was added to a full-scale DWDS[69]. Full-length 16S sequences taxonomically annotated as opportunistic pathogen species included *L. pneumophila*, *M. avium* and *M. barrasiae*. These were however relative minorities within their genera in DPS1, both before and after the end of chloramination (Supplementary Table 2).

The post-chloramination microbiome

The post-MCA core community of the DWDS was defined as taxa that were present at all sampling locations in the DWDS at the last sampling occasion in this study, when DWDS microbial communities were expected to have stabilized following the end of chloramination (Fig. 6). The relative abundance of the post-MCA core community was highest at DPN (42.5–43.1%) and DPS1 (32.2–45.8%), followed by DPS2 (20.7–35.0%), and lowest at DPE

(4.76–12.1%). Of the ASVs in this community, 31% were detected in the chloraminated system. Genera *Cereibacter*, *Haliangium*, *Hyphomicrobium* and *Methylotenera* were abundant members of the post-MCA community, although a large proportion of taxa identified could not be annotated to genus level. Many of these taxa belong to the newly proposed superphylum *Patescibacteria*[70], specifically classes *Parcubacteria* and *Gracilibacteria* (Supplementary Fig. 5). The new core community did not contain any taxonomic groups including known opportunistic pathogens.

Due to the ultrafiltration process in the WTP feeding this system, the only source of new taxa in this system is the biofilm. While *Hyphomicrobium* remained abundant, previous studies examining the biofilm community of this system did not detect *Cereibacter*, *Haliangium*, *Methylotenera* or *Patescibacteria*[17,27], perhaps suggesting that these were previously rare taxa below the resolution of the applied sequencing approaches, or that they have migrated from uncharacterized sections of this DWDS. The use of different taxonomic databases (Silva in this study, GreenGenes in previous studies), however, may also explain their lack of detection. *Cereibacter* is a newly proposed genus intended to include phototrophic members of genus *Gemmobacter*[71], several members of which degrade C1 compounds[72] which is also true for genera *Hyphomicrobium* and *Methylotenera*[73]. Metagenome-assembled genomes from *Patescibacteria* indicate broad capabilities to metabolize simple carbohydrates but very limited metabolism of more complex substrates[74]. *Patescibacteria* are believed to have fermentative lifestyles with limited biosynthetic capabilities, necessitating parasitic or symbiotic relationships with other microorganisms, although strict host ranges are unlikely[75]. Although metabolism is reduced in general, many possess capabilities to degrade complex compounds such as starch, chitin, and polyphenolics[75]. The end products of their fermentation could thus support other heterotrophic bacteria in the DWDS, as they are believed to do in groundwater environments[76] and thermokarst lakes[77]. Genus *Haliangium* belongs to *Myxobacteria*[78], a group of predatory bacteria. In the absence of MCA, *Haliangium* may be one aspect of biological control of regrowth in this DWDS.

In general, the new core community appeared to be oriented towards the metabolism of the specific organic matter profile of the water produced by this treatment plant. Without the addition of chloramine, the ultrafiltration combined with coagulation process applied in this specific treatment plant would provide only neutral, low molecular weight organic matter or low molecular weight humic substances[17,79] to be metabolized within the DWDS.

In conclusion, as distribution of ultrafiltered water facilitated observation of the biofilm using water samples, the response of this microbial community to the end of chloramination could be observed. A community shift from nitrification-based chemolithoautotrophy to heterotrophy and an increase of total and intact cell concentrations characterized the transition to a unchloraminated system. That this was not linked with indications of increased immediate biological risk can support drinking water producers considering making changes in their usage of secondary disinfectants.

This study has described microbial ecology linked to chloramination in drinking water distribution system biofilms, and the processes that occur when this ecosystem was disturbed. The emergence of conditionally rare taxa in the disinfectant-free environment highlights the need for deeper understanding of DWDS biofilm microbial ecology, and the role and potential of rare taxa to enter and flourish in the water phase following environmental change. While the conditionally rare taxa present in this study are unlikely to be hazardous to human health, the conditions in which pathogenic microorganisms can become the dominant members of the bulk water microbial community need to be understood, as eliminating even rare occurrences of certain pathogens from biofilm is likely difficult. Deep sequencing of a single sample from the English Channel contained 95% of the observed taxonomic units detected in shallow sequenced samples collected over a period of 6 years[80], suggesting deep sequencing of pipe biofilms from different materials and water exposure would be necessary to determine the extent to which rare taxa of concern could be present in full-scale drinking water distribution systems.

METHODS

Study site and sampling

Samples were collected in the Kvarnagården DWDS of Varberg, Sweden, which is maintained by Vatten och Miljö i Väst AB (Vivab). The source water is a mix of 80% surface water from the lake Stora Neden and 20% groundwater. Prior to distribution, the water was subjected to the following treatment steps: rapid sand filtration, coagulation and ultrafiltration, pH adjustment, chloramination, and UV-disinfection. MCA was added to a total chlorine concentration of 0.13–0.21 mg/l in the finished water. As of January 20th 2020, however, no MCA is added to the finished water.

Sampling locations were chosen to reflect a variety of locations and retention times within the DWDS. Regular sampling for FCM was performed at 6 locations in the DWDS as well as of the outgoing water from the DWTP. The sampling points in the DWDS were named after their position relative to the DWTP. The northern sampling point (DPN) is characterized by relatively long distance, yet very low residence time. The eastern (DPE) and southern (DPS1-3) sampling points are more proportional between distance and residence time. DPS2 is downstream of DPS1, and DPS3 is downstream of DPS2. The western sampling (DPW) point has a very low residence time. Samples for DNA sequencing were not collected from DPW. Details regarding the residence times and distances from the DWTP for the sampling points are available in Table 1.

Samples were taken for sequencing analyses on six occasions: two occasions before and four after the end of chloramination respectively: November and December 2019, March, April, May 2020 and February 2021.

Samples for FCM were collected in 15 mL Falcon tubes with the addition of 1% (v/v) sodium thiosulfate (20 g/l) to quench residual chlorine in samples before January 2020. Samples were transported at 4 °C and analyzed within 8 h.

Samples for sequencing were collected in borosilicate bottles (Merck, Germany) washed with sodium hypochlorite and rinsed thoroughly with MilliQ-filtered water. Between 1 and 10 l of water were filtered through 0.22 µm filter papers (Merck, Germany), depending on TCC. to ensure that at least 10^5 cells were present on each filter paper. Filter papers were put into sterile petri dishes and stored at −20 °C until DNA extraction. As the water was

Table 1. Residence time and distance from DWTP for sampling locations.

Sampling point	Residence time (h)	Distance from DWTP (km)
DPN	41[a]	17
DPE	45[a]	6.2
DPS1	10–20[b]	5.6
DPS2	32[a]	16
DPS3	>32[b]	21
DPW	17[a]	4.8
WTP	0.0–0.5[b]	0

[a]Estimated from hydraulic modeling by producer.
[b]Estimated based on location in the DWDS.

ultrafiltered prior to distribution, observed bulk water communities are expected to reflect the biofilm communities present in upstream pipe regions.

Samples for conventional water quality analyses were handled by Eurofins (first two sampling occasions) and SYNLAB (the remaining four sampling occasions). Samples were handled according to international standard methods provided by the laboratories. Values of select water quality parameters for sequenced samples are available as Supplementary Table 5.

Flow cytometry

FCM analysis was performed according to the protocol in Prest et al., 2014[81]. A BD Accuri C6 Plus instrument (Becton Dickinson, Belgium) with a 50 mW laser equipped was used to run the analyses. Every day of analysis, the instrument was checked by running a quality control of BD CSample Beads (Becton Dickinson, Belgium). Samples were stained with SYBR Green I (Invitrogen AG, Switzerland) by diluting 10 000× stock solution to 100× with dimethyl sulphoxide and then adding 5 µl to a final concentration of 1×. Intact cells were measured by adding 3 mM propidium iodide (Sigma Aldrich, Germany) into the SYBR Green I mixture. After incubation for 15 min in the dark in 37 °C, the samples were run as triplicates on flow rate 35 µl/min with a green fluorescence threshold of 500 arbitrary units.

Flow cytometric data was exported as FCS files to FlowJo software (Tree Star Inc, USA) for data processing. Events were detected with green fluorescence (FL-1, 533 +/− 30 nm) and red fluorescence (FL-3, >670 nm). Gating was performed on dot plots according to the strategy described[82] and applied identically on all analyzed samples.

Baseline models to describe seasonal fluctuations in TCC were generated by fitting sinusoidal functions to the data collected in 2018 and 2019. The following function was used with the lm-function in R.

$$\mathrm{TCC}_{\mathrm{model}}(t) = \alpha \cos\left(\frac{2\pi}{365}t\right) + \beta \sin\left(\frac{2\pi}{365}t\right) + \gamma \quad (1)$$

Where TCC_{model} is the modeled TCC (cells/ml), t is the time in days since January 1st, and α, β and γ are the fitted coefficients. The values of the coefficients for each sampling point are available in Supplementary Table 4. In order to verify the presence of structural breaks in the data following the end of chloramination, Chow tests were performed at all sampling points using the sctest function of the strucchange R package[83].

The extent to which growth was suppressed was quantified by subtracting the values generated by the baseline models from the TCC measured after the end of MCA addition.

$$\mathrm{TCC}_{\mathrm{added}}(t) = \mathrm{TCC}_{\mathrm{measured}}(t) - \mathrm{TCC}_{\mathrm{model}}(t) \quad (2)$$

Where $TCC_{measured}$ is the observed TCC after the end of chloramination at time t and TCC_{added} is the estimated number of cells added by ending chloramination (in other words, the residuals). TCC values measured >100 days after the end of chloramination were considered stable and were thus used to compute average cell additions for the sampling points. The average cell additions were presented together with 95% confidence intervals.

DNA extraction

Filter papers with concentrated cell material were cut into pieces and placed in the Lysing Matrix E (MP Biomedicals, USA) tube of the FastDNA Spin Kit for Soil. Using this kit and the manufacturer's instructions, DNA was extracted, then stored at −20 °C until further processing. Unused filter papers were extracted as negative controls.

V3-V4 region 16S rRNA gene sequencing

Amplicons of the V3–V4 region of the bacterial 16S rRNA gene were generated with universal bacterial primers Bact_341F (5′-CCTACGGGNGGCWGCAG-3′) and Bact_785R (5′-GACTACHVGGGTATCTAATCC-3′). Each PCR contained 12.2 µl MQ water, 10 µl 5PRIME HotMasterMix (Quantabio, USA), 0.8 µl Bovine Serum Albumin (10 mg/ml), 0.5 µl of both forward and reverse primers (10 µM) and 1 µl of DNA template. PCR amplification used 94 °C for 3 min; 35 cycles of 94 °C for 45 s; 50 °C for 1 min; 72 °C for 1.5 min with a finishing step of 72 °C for 10 min. Amplifications were performed in triplicate and pooled. Pooled amplicons from each PCR reaction were quantified with the Qubit 2.0 dsDNA HS Assay Kit (Thermo Fisher Scientific, USA) and inspected visually with agarose gel electrophoresis. 50 ng of each replicate of amplicons (same distribution point and time of sampling) were pooled together and purified with the QIAquick PCR Purification Kit (Qiagen, Germany) according to the manufacturer's instructions. Sequence analysis was performed with a MiSeq Reagent Kit v3 (Illumina, USA) and run 600 cycles with 5–15% PhiX according to the manufacturer's instructions. Negative controls, samples from the outgoing water from the DWTP and DPS3 did not have visible bands but were included in the run. These yielded low-quality sequences with high variability between replicates, and thus these sampling points were excluded from further analysis.

Full-length 16S rRNA gene sequencing

Amplicons spanning the V1 – V9 region of the bacterial 16S rRNA gene were generated with universal bacterial primers S-D-Bact-0008-c-S-20 (27F) (5′-AGRGTTYGATYMTGGCTCAG-3′) and S-D-Bact-1492-a-A-22 (1492R) (5′-TACGGYTACCTTGTTACGACTT-3′). Primer coverage was assessed using TestPrime 1.0 web interface and the Silva SSU 138.1 RefNR database[84]. Each PCR contained 9.75 µl MQ water, 12.5 µl 2× Terra PCR Direct Buffer, 0.5 µl/0,625 U Terra PCR Direct Polymerase Mix (Takara Bio USA Inc.), 0.625 µl of both forward and reverse primers (10 µM) and 1 µl DNA template. PCR was performed with an initial denaturation at 98 °C for 2 min, 35 cycles of 95 °C for 1 min, 60 °C for 1 min and 68 °C for 3 min and a final extension at 68 °C for 10 min. Amplicons from each PCR reaction were inspected visually with agarose gel electrophoresis, purified with 1,8x Agencourt AMPure XP magnetic beads (Beckman Coulter Inc. USA) and quantified with Qubit 2.0 dsDNA Assay (Thermo Fisher Scientific, USA). Library preparation and sequencing was performed with protocol for Native barcoding amplicons SQK-LSK109 with expansions EXP-NBD104 and EXP-NBD114 according to the instructions from the supplier and loaded on MinION R9.4 flow cell (Oxford Nanopore Technology, Oxford, UK).

V3-V4 region bioinformatics

Sequenced reads were demultiplexed using deML[85]. Following removal of adapter and primer sequences reads were demultiplexed and truncated at 250 bp for forward reads and 230 bp for reverse reads (settings trimLeft = c(5,5),maxN = 0, maxEE = c(2,2), truncQ = 2) prior to amplicon sequence variant (ASV) generation and chimera removal by DADA2[86], allowing for sufficient overlap to allow merging of forward and reverse reads. ASVs were taxonomically annotated using Silva (nr99/v138) database[87]. ASVs present in the negative control samples, and those represented by less than 20 reads in total, were removed from the dataset as to not include spurious sequences stemming from contamination or sequencing errors[84].

ASVs were aligned against each other using the DECIPHER package[88] for R. A phylogenetic tree was constructed from the aligned reads through use of the FastTree software[89], with the Jukes-Cantor model of nucleotide evolution and the "CAT" model approximation for evolution rates.

The ASV-table, taxonomic annotations and phylogenetic tree were joined in a phyloseq object in R. The packages phyloseq[90], dplyr[91] and tidyr[92] were used for data handling. The microbiome package[93] was used to calculate alpha diversity indexes and aggregate rare taxa. The vegan package[94] was used to assess beta diversity and create rarefaction curves. Beta dispersion within sampling points (based on the group centroid) was calculated using the betadisper function of the vegan package, and pairwise significance testing of these dispersions was done using the permutest function of the vegan package. Permutational multivariate anova (PERMANOVA) was performed using the adonis2 function of the vegan package. The psych package[95] was used to test for pairwise Spearman correlations (co-occurrence) between ASVs, with the Holm method of adjusting *p*-values for multiple tests. Only ASVs which were present in more than 20 samples were used, as including ASVs only present in a small number of samples may produce spurious correlations arising from large numbers of zeroes in the data[96]. The correlation matrix was converted into a network using the package igraph[97]; correlations with $|\rho| > 0.75$ and $p < 0.01$ were considered relevant. Co-occurrence networks were visualized using the GGally package[98]. All other graphs were generated through ggplot2[99]. Relative abundances of taxa were scaled by the TCC of the sample as determined by FCM[100].

Full-length 16S rRNA gene bioinformatics

Sequencer output was base called using the Guppy basecaller[101] (version 6.3.2+bb5453e) and minimap2[102] (version 2.22-r1101) with default settings except for the"sup" setting being enabled for more precise basecalling. Basecalled and demultiplexed fastq-files were then analyzed with respect to taxa clustering, taxonomic annotation and relative abundance/count data with the Emu[103] software and the default settings and database. The relative abundances and taxonomic annotations were imported into R and converted into a phyloseq object. Species with mean relative abundances below 0.001% were removed from the dataset. The packages phyloseq[90], dplyr[91] and purrr[104] were used for data handling.

DATA AVAILABILITY

Raw files are available on the Sequence Read Archive (SRA) of the National Center for Biotechnology (NCBI) under the project code PRJNA826279. Flow cytometry data is available upon reasonable request.

CODE AVAILABILITY

All codes used in this study are available from the corresponding author upon reasonable request.

Received: 28 November 2022; Accepted: 2 May 2023;
Published online: 17 May 2023

REFERENCES

1. Maki, J. S., LaCroix, S. J., Hopkins, B. S. & Staley, J. T. Recovery and diversity of heterotrophic bacteria from chlorinated drinking waters. *Appl. Environ. Microbiol.* **51**, 1047–1055 (1986).
2. Allen, M. J., Edberg, S. C. & Reasoner, D. J. Heterotrophic plate count bacteria—what is their significance in drinking water? *Int. J. Food Microbiol.* **92**, 265–274 (2004).
3. Allard, S., Kristiana, I., Andringa-Bate, C. & Joll, C. A. Alternative application of preformed monochloramine as a drinking water disinfectant for redosing in long drinking water distribution system servicing remote locations. *Water Res.* **185**, 116083 (2020).
4. Hua, G. & Reckhow, D. A. Comparison of disinfection byproduct formation from chlorine and alternative disinfectants. *Water Res.* **41**, 1667–1678 (2007).
5. Cunliffe, D. A. Bacterial nitrification in chloraminated water supplies. *Appl. Environ. Microbiol.* **57**, 3399–3402 (1991).
6. Maestre, J. P., Wahman, D. G. & Speitel, G. E. Monochloramine cometabolism by Nitrosomonas europaea under drinking water conditions. *Water Res.* **47**, 4701–4709 (2013).
7. Maestre, J. P., Wahman, D. G. & Speitel, G. E. Monochloramine cometabolism by mixed-culture nitrifiers under drinking water conditions. *Environ. Sci. Technol.* **50**, 6240–6248 (2016).
8. Dunnick, J. K. & Melnick, R. L. Assessment of the carcinogenic potential of chlorinated water: experimental studies of chlorine, chloramine, and trihalomethanes. *JNCI J. Natl Cancer Inst.* **85**, 817–822 (1993).
9. Rosario-Ortiz, F., Rose, J., Speight, V., Gunten, U. V. & Schnoor, J. How do you like your tap water? *Science* **351**, 912–914 (2016).
10. Regan, J. M., Harrington, G. W., Baribeau, H., Leon, R. D. & Noguera, D. R. Diversity of nitrifying bacteria in full-scale chloraminated distribution systems. *Water Res.* **37**, 197–205 (2003).
11. Daims, H. et al. Complete nitrification by Nitrospira bacteria. *Nature* **528**, 504–509 (2015).
12. Kindaichi, T., Ito, T. & Okabe, S. Ecophysiological interaction between nitrifying bacteria and heterotrophic bacteria in autotrophic nitrifying biofilms as determined by microautoradiography-fluorescence in situ hybridization. *Appl. Environ. Microbiol.* **70**, 1641–1650 (2004).
13. Zhang, Y., Love, N. & Edwards, M. Nitrification in drinking water systems. *Crit. Rev. Environ. Sci. Technol.* **39**, 153–208 (2009).
14. Liu, G. et al. Pyrosequencing reveals bacterial communities in unchlorinated drinking water distribution system: an integral study of bulk water, suspended solids, loose deposits, and pipe wall biofilm. *Environ. Sci. Technol.* **48**, 5467–5476 (2014).
15. Liu, G. et al. Assessing the origin of bacteria in tap water and distribution system in an unchlorinated drinking water system by SourceTracker using microbial community fingerprints. *Water Res.* **138**, 86–96 (2018).
16. Pinto, A. J., Xi, C. & Raskin, L. Bacterial community structure in the drinking water microbiome is governed by filtration processes. *Environ. Sci. Technol.* **46**, 8851–8859 (2012).
17. Pullerits, K. et al. Impact of coagulation–ultrafiltration on long-term pipe biofilm dynamics in a full-scale chloraminated drinking water distribution system. *Environ. Sci. Water Res. Technol.* **6**, 3044–3056 (2020).
18. Cruz, M. C., Woo, Y., Flemming, H.-C. & Wuertz, S. Nitrifying niche differentiation in biofilms from full-scale chloraminated drinking water distribution system. *Water Res.* **176**, 115738 (2020).
19. Potgieter, S. C. et al. Microbial nitrogen metabolism in chloraminated drinking water reservoirs. *mSphere* **5**, e00274–00220 (2020).
20. Liu, G. et al. 360-degree distribution of biofilm quantity and community in an operational unchlorinated drinking water distribution pipe. *Environ. Sci. Technol.* **54**, 5619–5628 (2020).
21. Chatzigiannidou, I., Props, R. & Boon, N. Drinking water bacterial communities exhibit specific and selective necrotrophic growth. *npj Clean. Water* **1**, 22 (2018).
22. Bian, K. et al. Spatial dynamics of bacterial community in chlorinated drinking water distribution systems supplied with two treatment plants: An integral study of free-living and particle-associated bacteria. *Environ. Int.* **154**, 106552 (2021).
23. Pinto, A. J. et al. Spatial-temporal survey and occupancy-abundance modeling to predict bacterial community dynamics in the drinking water microbiome. *mBio* **5**, e01135–01114 (2014).
24. Lynch, M. D. J. & Neufeld, J. D. Ecology and exploration of the rare biosphere. *Nat. Rev. Microbiol.* **13**, 217–229 (2015).
25. Gomez-Alvarez, V., Pfaller, S., Pressman, J. G., Wahman, D. G. & Revetta, R. P. Resilience of microbial communities in a simulated drinking water distribution system subjected to disturbances: role of conditionally rare taxa and potential implications for antibiotic-resistant bacteria. *Environ. Sci. Water Res. Technol.* **2**, 645–657 (2016).
26. Wingender, J. & Flemming, H.-C. Biofilms in drinking water and their role as reservoir for pathogens. *Int. J. Hyg. Environ. Health* **214**, 417–423 (2011).
27. Chan, S. et al. Bacterial release from pipe biofilm in a full-scale drinking water distribution system. *npj Biofilms Microbiomes* **5**, 9 (2019).
28. Gillespie, S. et al. Assessing microbiological water quality in drinking water distribution systems with disinfectant residual using flow cytometry. *Water Res.* **65**, 224–234 (2014).
29. Li, W. et al. Effect of disinfectant residual on the interaction between bacterial growth and assimilable organic carbon in a drinking water distribution system. *Chemosphere* **202**, 586–597 (2018).
30. Potgieter, S. et al. Long-term spatial and temporal microbial community dynamics in a large-scale drinking water distribution system with multiple disinfectant regimes. *Water Res.* **139**, 406–419 (2018).
31. Schleich, C. et al. Mapping dynamics of bacterial communities in a full-scale drinking water distribution system using flow cytometry. *Water* **11**, 2137 (2019).
32. Douterelo, I., Fish, K. E. & Boxall, J. B. Succession of bacterial and fungal communities within biofilms of a chlorinated drinking water distribution system. *Water Res.* **141**, 74–85 (2018).

33. Rochex, A., Godon, J.-J., Bernet, N. & Escudié, R. Role of shear stress on composition, diversity and dynamics of biofilm bacterial communities. *Water Res.* **42**, 4915–4922 (2008).
34. Williams, M. M., Santo Domingo, J. W. & Meckes, M. C. Population diversity in model potable water biofilms receiving chlorine or chloramine residual. *Biofouling* **21**, 279–288 (2005).
35. Bollmann, A. et al. Complete genome sequence of Nitrosomonas sp. Is79, an ammonia oxidizing bacterium adapted to low ammonium concentrations. *Stand. Genom. Sci.* **7**, 469–482 (2013).
36. Ushiki, N. et al. Nitrite oxidation kinetics of two Nitrospira strains: the quest for competition and ecological niche differentiation. *J. Biosci. Bioeng.* **123**, 581–589 (2017).
37. Gruber-Dorninger, C. et al. Functionally relevant diversity of closely related Nitrospira in activated sludge. *ISME J.* **9**, 643–655 (2015).
38. Koch, H. et al. Expanded metabolic versatility of ubiquitous nitrite-oxidizing bacteria from the genus Nitrospira. *Proc. Natl Acad. Sci.* **112**, 11371–11376 (2015).
39. Park, H. D. & Noguera, D. R. Nitrospira community composition in nitrifying reactors operated with two different dissolved oxygen levels. *J. Microbiol. Biotechnol.* **18**, 1470–1474 (2008).
40. Wang, Y. et al. Comammox in drinking water systems. *Water Res.* **116**, 332–341 (2017).
41. Pinto, A. J. et al. Metagenomic evidence for the presence of comammox nitrospira-like bacteria in a drinking water system. *mSphere* **1**, e00054–00015 (2016).
42. Brenner, D. J., Krieg, N. R., Staley, J. T. & Garrity, G. *Bergey's manual® of systematic bacteriology: volume two the proteobacteria part C the alpha-, beta-, delta-, and epsilonproteobacteria* (Springer, 2005).
43. Asaf, S., Numan, M., Khan, A. L. & Al-Harrasi, A. Sphingomonas: from diversity and genomics to functional role in environmental remediation and plant growth. *Crit. Rev. Biotechnol.* **40**, 138–152 (2020).
44. Bosso, L. & Cristinzio, G. A comprehensive overview of bacteria and fungi used for pentachlorophenol biodegradation. *Rev. Environ. Sci. Bio. Technol.* **13**, 387–427 (2014).
45. Sun, W., Liu, W., Cui, L., Zhang, M. & Wang, B. Characterization and identification of a chlorine-resistant bacterium, Sphingomonas TS001, from a model drinking water distribution system. *Sci. Total Environ.* **458-460**, 169–175 (2013).
46. Bereschenko, L. A., Stams, A. J. M., Euverink, G. J. W. & Loosdrecht, M. C. M. V. Biofilm formation on reverse osmosis membranes is initiated and dominated by Sphingomonas spp. *Appl. Environ. Microbiol.* **76**, 2623–2632 (2010).
47. Azeredo, J. & Oliveira, R. The role of exopolymers in the attachment of sphingomonas paucimobilis. *Biofouling* **16**, 59–67 (2000).
48. Tsuneda, S., Park, S., Hayashi, H., Jung, J. & Hirata, A. Enhancement of nitrifying biofilm formation using selected EPS produced by heterotrophic bacteria. *Water Sci. Technol.* **43**, 197–204 (2001).
49. Martineau, C., Mauffrey, F., Villemur, R. & Müller, V. Comparative analysis of denitrifying activities of Hyphomicrobium nitrativorans, Hyphomicrobium denitrificans, and Hyphomicrobium zavarzinii. *Appl. Environ. Microbiol.* **81**, 5003–5014 (2015).
50. Liu, H., Wahman, D. G. & Pressman, J. G. Evaluation of monochloramine and free chlorine penetration in a drinking water storage tank sediment using microelectrodes. *Environ. Sci. Technol.* **53**, 9352–9360 (2019).
51. Harder, W., Matin, A. & Attwood, M. M. Studies on the physiological significance of the lack of a pyruvate dehydrogenase complex in Hyphomicrobium sp. *Microbiology* **86**, 319–326 (1975).
52. Vuilleumier, S. et al. Complete genome sequence of the chloromethane-degrading Hyphomicrobium sp. strain MC1. *J. Bacteriol.* **193**, 5035–5036 (2011).
53. Matsumoto, S. et al. Microbial community structure in autotrophic nitrifying granules characterized by experimental and simulation analyses. *Environ. Microbiol.* **12**, 192–206 (2010).
54. Pick, F. C., Fish, K. E. & Boxall, J. B. Assimilable organic carbon cycling within drinking water distribution systems. *Water Res.* **198**, 117147 (2021).
55. Liu, Y.-X., Qin, Y. & Bai, Y. Reductionist synthetic community approaches in root microbiome research. *Curr. Opin. Microbiol.* **49**, 97–102 (2019).
56. Vrancken, G., Gregory, A. C., Huys, G. R. B., Faust, K. & Raes, J. Synthetic ecology of the human gut microbiota. *Nat. Rev. Microbiol.* **17**, 754–763 (2019).
57. Newton, R. J., Jones, S. E., Eiler, A., McMahon, K. D. & Bertilsson, S. A guide to the natural history of freshwater lake bacteria. *Microbiol. Mol. Biol. Rev.* **75**, 14–49 (2011).
58. Schleich, C., Paul, C. J., Rådström, P. & Keucken, A. In *Abstract, IWA Specialist Conference: Disinfection and DBPs* (Milan, Italy, 2022).
59. Wu, X. et al. Culturing of "unculturable" subsurface microbes: natural organic carbon source fuels the growth of diverse and distinct bacteria from groundwater. *Front. Microbiol.* **11**, 610001–610001 (2020).
60. Sack, E. L. W., Van Der Wielen, P. W. J. J. & Van Der Kooij, D. Utilization of oligo- and polysaccharides at microgram-per-litre levels in freshwater by Flavobacterium johnsoniae. *J. Appl. Microbiol.* **108**, 1430–1440 (2010).
61. van der Kooij, D. & Hijnen, W. A. Nutritional versatility of a starch-utilizing Flavobacterium at low substrate concentrations. *Appl. Environ. Microbiol.* **45**, 804–810 (1983).
62. Mookherjee, A. & Jurkevitch, E. Interactions between Bdellovibrio and like organisms and bacteria in biofilms: beyond predator–prey dynamics. *Environ. Microbiol.* **24**, 998–1011 (2022).
63. Sockett, R. E. Predatory lifestyle of Bdellovibrio bacteriovorus. *Annu. Rev. Microbiol.* **63**, 523–539 (2009).
64. Koval, S. F. et al. Bdellovibrio exovorus sp. nov., a novel predator of Caulobacter crescentus. *Int. J. Syst. Evolut. Microbiol.* **63**, 146–151 (2013).
65. Kadouri, D. & O'Toole, G. A. Susceptibility of biofilms to Bdellovibrio bacteriovorus attack. *Appl. Environ. Microbiol.* **71**, 4044–4051 (2005).
66. Varon, M. & Zeigler, B. P. Bacterial predator-prey interaction at low prey density. *Appl. Environ. Microbiol.* **36**, 11–17 (1978).
67. Bautista-de los Santos, Q. M. et al. Emerging investigators series: microbial communities in full-scale drinking water distribution systems – a meta-analysis. *Environ. Sci. Water Res. Technol.* **2**, 631–644 (2016).
68. European Parliament. Directive (EU) 2020/2184 of the European Parliament and of the Council of 16 December 2020 on the quality of water intended for human consumption. (2020).
69. Chiao, T.-H., Clancy, T. M., Pinto, A., Xi, C. & Raskin, L. Differential resistance of drinking water bacterial populations to monochloramine disinfection. *Environ. Sci. Technol.* **48**, 4038–4047 (2014).
70. Rinke, C. et al. Insights into the phylogeny and coding potential of microbial dark matter. *Nature* **499**, 431–437 (2013).
71. Suresh, G., Sasikala, C. & Ramana, C. V. Reclassification of Gemmobacter changlensis to a new genus as Cereibacter changlensis gen. nov., comb. nov. *Int. J. Syst. Evolut. Microbiol.* **65**, 794–798 (2015).
72. Kröber, E. et al. Comparative genomics analyses indicate differential methylated amine utilization trait within members of the genus Gemmobacter. *Environ. Microbiol. Rep.* **13**, 195–208 (2021).
73. Chistoserdova, L., Kalyuzhnaya, M. G. & Lidstrom, M. E. The expanding world of methylotrophic metabolism. *Annu. Rev. Microbiol.* **63**, 477–499 (2009).
74. Tian, R. et al. Small and mighty: adaptation of superphylum Patescibacteria to groundwater environment drives their genome simplicity. *Microbiome* **8**, 51 (2020).
75. Chaudhari, N. M. et al. The economical lifestyle of CPR bacteria in groundwater allows little preference for environmental drivers. *Environ. Microbiome* **16**, 24 (2021).
76. Mehrshad, M. et al. Energy efficiency and biological interactions define the core microbiome of deep oligotrophic groundwater. *Nat. Commun.* **12**, 4253 (2021).
77. Adrien, V. et al. Ultra-small and abundant: candidate phyla radiation bacteria are potential catalysts of carbon transformation in a thermokarst lake ecosystem. *Limnol. Oceanogr. Lett.* **5**, 212–220 (2020).
78. Muñoz-Dorado, J., Marcos-Torres, F. J., García-Bravo, E., Moraleda-Muñoz, A. & Pérez, J. Myxobacteria: moving, killing, feeding, and surviving together. *Front. Microbiol.* **7**, 781 (2016).
79. Huber, S. A., Balz, A., Abert, M. & Pronk, W. Characterisation of aquatic humic and non-humic matter with size-exclusion chromatography – organic carbon detection – organic nitrogen detection (LC-OCD-OND). *Water Res.* **45**, 879–885 (2011).
80. Caporaso, J. G., Paszkiewicz, K., Field, D., Knight, R. & Gilbert, J. A. The Western English Channel contains a persistent microbial seed bank. *ISME J.* **6**, 1089–1093 (2012).
81. Prest, E. I. et al. Combining flow cytometry and 16S rRNA gene pyrosequencing: a promising approach for drinking water monitoring and characterization. *Water Res.* **63**, 179–189 (2014).
82. Prest, E. I., Hammes, F., Kötzsch, S., van Loosdrecht, M. C. M. & Vrouwenvelder, J. S. Monitoring microbiological changes in drinking water systems using a fast and reproducible flow cytometric method. *Water Res.* **47**, 7131–7142 (2013).
83. Zeileis, A., Leisch, F., Hornik, K. & Kleiber, C. strucchange: an R package for testing for structural change in linear regression models. *J. Stat. Softw.* **7**, 1–38 (2002).
84. Klindworth, A. et al. Evaluation of general 16S ribosomal RNA gene PCR primers for classical and next-generation sequencing-based diversity studies. *Nucleic Acids Res.* **41**, e1–e1 (2013).
85. Renaud, G., Stenzel, U., Maricic, T., Wiebe, V. & Kelso, J. deML: robust demultiplexing of Illumina sequences using a likelihood-based approach. *Bioinformatics* **31**, 770–772 (2015).
86. Callahan, B. J. et al. DADA2: high-resolution sample inference from Illumina amplicon data. *Nat. Methods* **13**, 581–583 (2016).
87. Quast, C. et al. The SILVA ribosomal RNA gene database project: improved data processing and web-based tools. *Nucleic Acids Res.* **41**, D590–D596 (2013).
88. Wright, E. S. RNAconTest: comparing tools for noncoding RNA multiple sequence alignment based on structural consistency. *RNA* **26**, 531–540 (2020).

89. Price, M. N., Dehal, P. S. & Arkin, A. P. FastTree 2 – approximately maximum-likelihood trees for large alignments. *PLOS One* **5**, e9490 (2010).
90. McMurdie, P. J. & Holmes, S. phyloseq: an R package for reproducible interactive analysis and graphics of microbiome census data. *PLOS One* **8**, e61217 (2013).
91. dplyr: a grammar of data manipulation. https://dplyr.tidyverse.org (2022).
92. tidyr: tidy messy data. https://tidyr.tidyverse.org (2022).
93. Tools for microbiome analysis in R. http://microbiome.github.com/microbiome (2017).
94. Oksanen, J. et al. vegan: community ecology package. https://CRAN.R-project.org/package=vegan (2020).
95. psych: procedures for psychological, psychometric, and personality research. https://CRAN.R-project.org/package=psych (2021).
96. Weiss, S. et al. Correlation detection strategies in microbial data sets vary widely in sensitivity and precision. *ISME J.* **10**, 1669–1681 (2016).
97. Csardi, G. & Nepusz, T. The igraph software package for complex network research. *Inter J. Complex Syst.* **1695**, 1–9 (2006).
98. GGally: Extension to 'ggplot2'. https://ggobi.github.io/ggally/ (2021).
99. Wickham, H. *ggplot2: elegant graphics for data analysis*. https://ggplot2.tidyverse.org (Springer, 2016).
100. Props, R. et al. Absolute quantification of microbial taxon abundances. *ISME J.* **11**, 584–587 (2017).
101. Guppy basecalling software. https://community.nanoporetech.com (2022).
102. Li, H. Minimap2: pairwise alignment for nucleotide sequences. *Bioinformatics* **34**, 3094–3100 (2018).
103. Curry, K. D. et al. Emu: species-level microbial community profiling of full-length 16S rRNA Oxford Nanopore sequencing data. *Nat. Methods* **19**, 845–853 (2022).
104. purrr: functional programming tools. https://purrr.tidyverse.org/ (2020).
105. Attwood, M. M. & Harder, W. A rapid and specific enrichment procedure for-Hyphomicrobium spp. *Antonie van. Leeuwenhoek* **38**, 369–377 (1972).
106. Meiklejohn, J. The isolation of Nitrosomonas europaea in pure culture. *Microbiology* **4**, 185–191 (1950).
107. Ehrich, S., Behrens, D., Lebedeva, E., Ludwig, W. & Bock, E. A new obligately chemolithoautotrophic, nitrite-oxidizing bacterium,Nitrospira moscoviensis sp. nov. and its phylogenetic relationship. *Arch. Microbiol.* **164**, 16–23 (1995).
108. Daugulis, A. J. & McCracken, C. M. Microbial degradation of high and low molecular weight polyaromatic hydrocarbons in a two-phase partitioning bioreactor by two strains of Sphingomonas sp. *Biotechnol. Lett.* **25**, 1441–1444 (2003).

AUTHOR CONTRIBUTIONS

T.R. performed bioinformatics and drafted the manuscript. M.D. contributed to sampling, FCM analysis, DNA extraction and manuscript revisions. C.S. contributed to sampling, FCM analysis and manuscript revisions. J.A. and B.B. assisted with bioinformatics. I.D. and E.N.S performed amplicon sequencing. K.P., D.S., M.F., facilitated the study with intellectual contributions and manuscript review, A.K., P.R. and C.J.P. designed the study, managed different stages of the project and provided feedback for manuscript revisions. All authors approved the final manuscript.

FUNDING

This study was funded by the Swedish Water Development fund (SVU), Sweden Water Research AB the DRICKS center for Drinking Water Research, The Swedish Civil Contingencies Agency (MSB) and the public joint-stock utilities Vatten & Miljö i Väst AB (VIVAB) and Norrvatten AB. Open access funding provided by Lund University.

COMPETING INTERESTS

The authors declare no competing interests.

ADDITIONAL INFORMATION

Supplementary information The online version contains supplementary material available at https://doi.org/10.1038/s41545-023-00253-x.

Correspondence and requests for materials should be addressed to Catherine J. Paul.

Reprints and permission information is available at http://www.nature.com/reprints

Publisher's note Springer Nature remains neutral with regard to jurisdictional claims in published maps and institutional affiliations.